Analog Integr Circ Sig Process (2009) 60:57–70
DOI 10.1007/s10470-008-9219-0

Performance analysis of burst-mode receivers with clock phase alignment and forward error correction for GPON

Bhavin J. Shastri · Julien Faucher · Noha Kheder · Ming Zeng · Nicholas Zicha · David V. Plant

Received: 15 December 2007 / Revised: 20 August 2008 / Accepted: 20 August 2008 / Published online: 11 October 2008

Abstract We experimentally demonstrate the performance analysis of burst-mode receivers (BMRx) in a 622 Mb/s 20-km gigabit-capable passive optical network (GPON) uplink. Our receiver features automatic phase acquisition using a clock phase aligner (CPA), and forward-error correction using (255, 239) Reed-Solomon (RS) codes. The BMRx provides instantaneous (0 preamble bit) phase acquisition and a packet-loss ratio (PLR) $< 10^{-6}$ for any phase step ($\pm 2\pi$ rads) between consecutive packets, while also supporting more than 600 consecutive identical digits (CIDs). The receiver also accomplishes a 3-dB coding gain at a bit-error rate (BER) of 10^{-10}. The CPA makes use of a phase picking algorithm and an oversampling clock-and-data recovery circuit operated at $2\times$ the bit rate. The receiver meets the GPON physical media dependent layer specifications defined in the ITU-T recommendation G.984.2 standard. We investigate the PLR performance of the system and quantify it as a function of the phase step between consecutive packets, received signal power, CID immunity, and BER, while also assessing the tradeoffs in preamble length, power penalty, and pattern correlator error resistance. We also study the impact of mode-partition noise in the GPON uplink in terms of the effective PLR and BER coding gain performance of the system. In addition, we demonstrate how the CPA and the RS(255, 239) codes can be used in tandem for dynamic burst-error correction giving reliable BERs in bursty channels.

Keywords Burst-mode receiver · Clock-and-data recovery · Clock phase alignment · Forward-error correction · Gigabit passive optical network · Mode-partition noise · Packet-loss ratio

1 Introduction

Passive optical networks (PONs) are an emerging optical multi-access network technology based on all-optical core. PONs are expected to solve the so-called "first and last mile problem" that remains a bottleneck between the backbone network and high-speed local area networks (LANs) [1–4]. PONs provide a low-cost solution, with a guaranteed quality of service (QoS) of deploying fiber-to-the-premises/cabinet/building/home/user (FTTx) [5]. FTTx is an effective solution to enable new multimedia services such as interactive video, voice, image, audio, and fast Internet [6].

Figure 1 shows an example of a gigabit-capable PON (GPON) network. In the downstream direction, the network is point-to-point (P2P). Continuous data are broadcast from the optical line terminal (OLT) to the optical network units (ONUs) using time division multiplexing (TDM) in the 1480–1550-nm wavelength band. The transmit side of the OLT and the receive side of the ONUs can therefore use continuous mode ICs. The challenge in the design of a chip set for PONs comes from the upstream data path. In the upstream direction, the network is point-to-multipoint

Special Issue: IEEE Midwest Symposium on Circuits and Systems (MWSCAS)/Northeast Workshop on Circuits and Systems (NEWCAS) 2007.

B. J. Shastri (✉) · N. Kheder · M. Zeng · N. Zicha · D. V. Plant
Photonic Systems Group, Department of Electrical & Computer Engineering, McGill University, Montreal, QC, Canada H3A 2A7
e-mail: shastri@ieee.org

J. Faucher
PMC-Sierra, Inc., Ville Mont-Royal, QC, Canada H3R 3L5

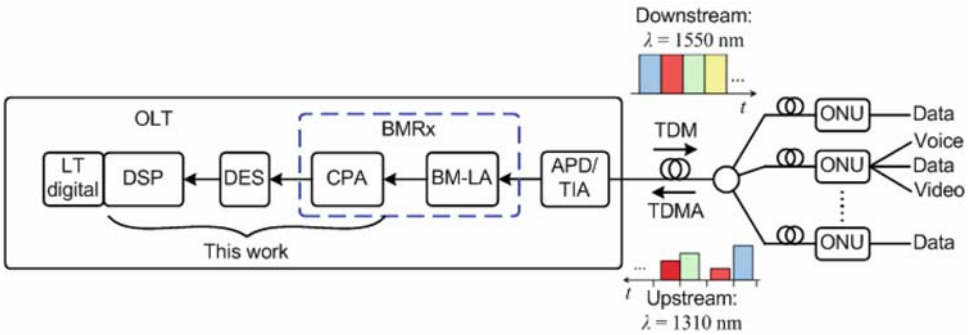

Fig. 1 Generic GPON network for FTTx showing our work on BMRx in context (OLT: optical line terminal; LT: line terminator; DSP: digital signal processing; DES: deserializer; BMRx: burst-mode receiver; CPA: clock phase aligner; BM-LA: burst-mode limiting amplifier; APD: avalanche photodiode; TIA: transimpedance amplifier; TDM: time division multiplexing; TDMA: time division multiple access; ONU: optical network unit)

(P2MP); using time division multiple access (TDMA), multiple ONUs transmit bursty data in the 1310-nm window to the OLT in the central office (CO). To use the shared medium effectively, the ONUs require a burst-mode transmitter with a short turn-on/off delay [7]. Because of optical path differences in the upstream path, packets can vary in phase and amplitude. To deal with these variations, the OLT requires a burst-mode receiver (BMRx). The BMRx is responsible for amplitude and phase recovery, which must be achieved at the beginning of every packet. At the front-end of the BMRx is a burst-mode limiting amplifier (BM-LA) responsible for amplitude recovery. Then, clock-and-data recovery (CDR) is performed with phase acquisition by a clock phase aligner (CPA). The most important characteristic of the CPA is its phase acquisition time which must be as short as possible. This paper focuses on the CPA aspect of the BMRx.

Current PON systems employ Fabry-Perot (FP) lasers, a multi-longitudinal mode (MLM) device, at the ONU to minimize the cost per subscriber. FP lasers provide the most cost effective solution for meeting the PON requirements, by having the optimum optical power required for a 20-km reach in the 1310–1550-nm range. However, the bit-error rate (BER) and the packet-loss ratio (PLR) performance of the optical system may be severely impaired by the mode-partition noise (MPN) of the FP laser coupled with the chromatic dispersion that exists in the transmission fiber [8]. Thus, MPN introduces a limitation on the length of the optical link. Consequently, the GPON physical media dependent (PMD) layer specifications defined in the International Telecommunication Union (ITU-T) recommendation G.984.2 standard [9], proposes the use of error-correcting codes (ECC) to reduce the associated penalty.

Another problem which inherently arises in a GPON uplink is that of burst-errors (clustered bit errors) due to the phase acquisition process by CDRs for bursty and packet-mode data. This makes BER measurements unreliable and unpredictable. In particular, a sudden phase step between consecutive packets can induce a severely errored burst, making the BER convergence difficult. Thus, the BER can change from measurement to measurement for the same signal-to-noise ratio (SNR) depending on the relative phase difference between consecutive packets.

Recently, we demonstrated standalone receivers for PON applications [10, 11]. However, the results presented were based on an emulated PON electrical test-bed. Although, useful in validating the proof-of-concept, these results do not give an insight on the performance of these receivers in a realistic PON test-bed.

In this paper, we experimentally investigate the effect of channel impairments on the performance of a BMRx in a 622 Mb/s 20-km GPON uplink. The receiver features automatic phase acquisition using a CPA, and forward-error correction (FEC). The CPA and the FEC improve the PLR performance and the BER performance of the system, respectively. More specifically, the BMRx provides instantaneous (0-bit) phase acquisition for any phase step ($\pm 2\pi$ rads) between consecutive packets with PLR $< 10^{-6}$ and BER $< 10^{-10}$. The receiver also accomplishes a 3-dB coding gain at a BER $= 10^{-10}$. The CPA makes use of a phase picking algorithm and an oversampling CDR operated at $2\times$ the bit rate. FEC is employed by using (255, 239) Reed-Solomon (RS) codes.

The instantaneous phase acquisition reduces the burst-mode sensitivity penalty of the receiver [12, 13], and also increases the effective throughput of the system by increasing the information rate. The coding gain can be used to reduce the minimum and maximum transmitter power, or increase the minimum receiver sensitivity by the same amount. Alternatively, the effective coding gain can be used to reduce the penalty due to MPN, and thus achieve

a longer physical reach or support more splits per single PON tree. Our BMRx meets the GPON PMD layer specifications as specified in the G.984.2 standard [9].

We also study the impact of MPN in the uplink in terms of the effective BER and PLR coding gain. We investigate the PLR performance of the system and quantify it as a function of the phase step between consecutive packets, received signal power, consecutive identical digits (CIDs) immunity, and BER. We also assess the tradeoffs in preamble length, power penalty, and pattern correlator error resistance. In addition, we demonstrate how the CPA and the RS(255, 239) codes can be used in conjunction to account for dynamic burst-error correction giving reliable BERs in bursty channels. These results will help refine theoretical models of BMRx and PONs, and provide input for establishing realistic power budgets.

The rest of the paper is organized as follows. In Sect. 2, we present the GPON experimental setup. The design and implementation of the BMRx is described in Sect. 3. Section 4 is devoted to the presentation and analysis of the experimental results. Finally, the paper is summarized and concluded in Sect. 5.

2 GPON experimental setup

A block diagram of the GPON uplink experimental setup is shown in Fig. 2. A 1310-nm laser is modulated with upstream PON traffic using an electro-optic modulator (EOM). The modulated signal is then sent through 20 km of uplink single-mode fiber (SMF-28). The desired information rate is 622 Mb/s. As the RS(255, 239) code introduces $\sim$15/14 overhead, we use an aggregate bit rate of 666.43 Mb/s. A variable optical attenuator (VOA) serves to control the received power level. The optical to electrical conversion is performed by a photodetector. The electrical signal is then low-pass filtered (LPF) by a fourth-order Bessel-Thomson filter whose -3-dB cutoff frequency is $0.7\times$ bit rate, or 467 MHz. Such a filter has an optimum bandwidth to filter out noise while keeping inter-symbol interference (ISI) to a minimum [14].

A typical bursty signal that complies with PON standards is used as a test signal in our experiments and is depicted in Fig. 3. Packet 1 serves as a dummy packet to force the burst-mode CDR to lock to a certain phase ϕ_1 before the arrival of packet 2 with phase ϕ_2. The BER and PLR measurements are performed on packet 2 only. Packet 2 consists of 16 guard bits, 0–28 (l) preamble bits, 20 delimiter bits, $2^{15}-1$ payload bits, and 48 comma bits. The guard, preamble, and delimiter bits correspond to the physical-layer upstream burst-mode overhead of 8 bytes at 622 Mb/s as specified by the G.984.2 standard [9]. The guard bits provide distance between two consecutive packets to avoid collisions. The preamble is split into two fields, a threshold determination field (TDF) for amplitude recovery and a CPA field for clock-phase recovery. The delimiter is a unique pattern indicating the start of the packet to perform byte synchronization. Likewise, the comma is a unique pattern to indicate the end of the payload. The payload is simply a non-return-to-zero (NRZ) $2^{15}-1$ pseudorandom binary sequence (PRBS). The PLR and the BER are measured on the payload bits only. We define the lock acquisition time corresponding to the number of bits (l) needed in front of the delimiter in order to get error-free operation, that is, a zero PLR for over 3 min of operation at 622 Mb/s ($>10^6$ packets received, i.e., PLR $< 10^{-6}$), a BER $< 10^{-10}$, and for any phase step ($-2\pi \le \Delta\varphi \le +2\pi$ rads) between consecutive packets. The GPON compliant OLT requires a preamble length of no more than 28 bits. We will demonstrate that even at $l = 0$ (no preamble bits), we achieve error-free operation, allowing for instantaneous phase acquisition.

This bursty upstream PON traffic is generated by adjusting the phase between alternating packets from two programmable ports of an HP80000 pattern generator, which are then concatenated via a radio frequency (RF) power combiner (PC), and used to drive the EOM (see Fig. 2). A silence period T_s, consisting of a phase step $|\Delta\varphi| \le 2\pi$ rads, and an all-zero sequence of m CIDs can be inserted between the packets. The silence period can be expressed as

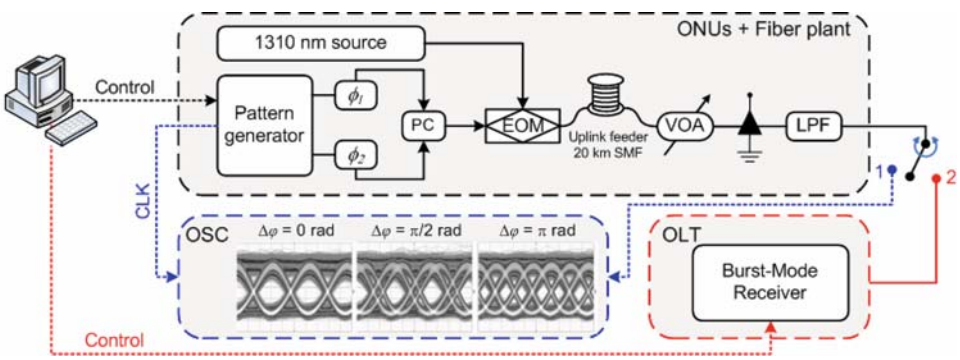

Fig. 2 Experimental setup for a GPON uplink (CLK: clock; PC: power combiner; EOM: electro-optic modulator; SMF: single-mode fiber; VOA: variable optical attenuator; LPF low-pass filter; ONU: optical network unit; OLT: optical line terminal; OSC: oscilloscope)

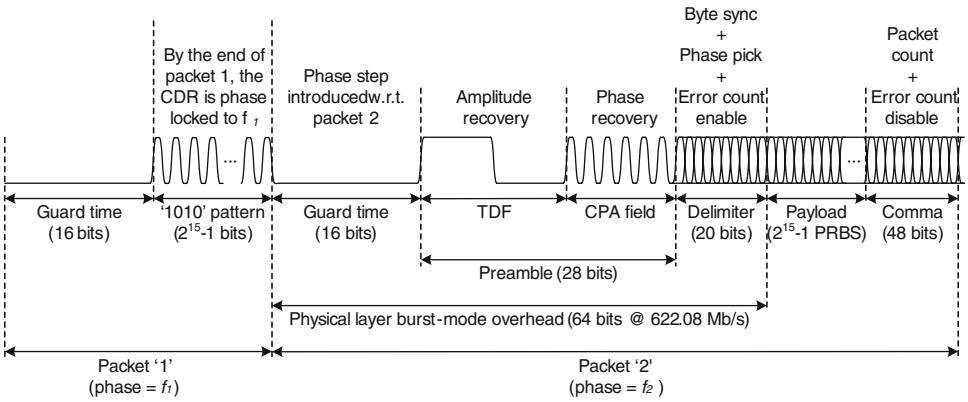

Fig. 3 Typical burst-mode uplink test signal and specification at 622 Mb/s (TDF: threshold determination field; CPA: clock phase alignment; PRBS: pseudorandom binary sequence)

$$T_s = \left(m + \frac{\Delta\varphi}{2\pi}\right)T \tag{1}$$

where T is the bit period. The phase step between the consecutive packets can be set anywhere between ± 2 ns with a 2-ps resolution, corresponding to a ± 1.25 unit interval (UI) at ~ 622 Mb/s. Note that 1 UI corresponds to a 1-bit period. Eye diagrams of the bursty traffic input to the BMRx are shown in Fig. 2 with different phases: $\Delta\varphi = 0$ rad (0 ps), $\Delta\varphi = \pi/2$ rads (400 ps), and $\Delta\varphi = \pi$ rads (800 ps).

3 GPON burst-mode receiver

3.1 Building blocks

The main building blocks of the GPON BMRx we designed are illustrated in Fig. 4. The receiver includes a multi-rate SONET CDR from Analog Devices (Part #ADN2819), a 1:8 deserializer from Maxim-IC (Part #MAX3885), and a CPA module and an FEC RS(255, 239) decoder implemented on a Virtex II Pro field-programmable gate array (FPGA) from Xilinx. The multirate CDR recovers the clock and data from the incoming signal. The CDR supports the following frequencies of interest: 622 Mb/s (without FEC), 666.43 Mb/s (with FEC), and 1.25 Gb/s. The latter frequency provides $2\times$ oversampling. Oversampling, together with the phase picking algorithm that will be described later, provide the core of the burst-mode CDR. The CDR is followed by a 1:8 deserializer (Des) that reduces the frequency of the recovered clock and data to a frequency that can be processed by the digital logic. The lower rate parallel data is then sent to the FPGA for further processing. Thereafter, a framer, a comma detector, the CPA (including byte synchronizers and a phase picker), phase-locked loops (PLLs), and the RS(255, 239) decoder are implemented on the FPGA alongside a custom BER tester (BERT). A computer is used to control the output of the pattern generator and to communicate with the FPGA on the receiver (see Fig. 2). Automatic detection of the payload is implemented on the FPGA through a framer and a comma detector, which are responsible for detecting the beginning (delimiter bits) and the end (comma bits) of the packet, respectively. The CPA makes use of a phase picking algorithm in [10] and the CDR operating at $2\times$ oversampling. The CPA is turned ON for the PLR measurements with phase acquisition for burst-mode reception when $\Delta\varphi \neq 0$ rad; otherwise, it can be bypassed for continuous-mode reception when $\Delta\varphi = 0$ rad. The CPA is then followed by the RS decoder and the FPGA-based BERT.

3.2 Burst-mode receiver functionalities

The idea behind the CPA is based on a simple, fast, and effective algorithm. Since the CDR samples the data twice per bit, the odd samples and even samples (O and E, respectively, in Fig. 4), sampled on the alternate (odd and even) clock rising edges (t_{odd} and t_{even} in Fig. 8) are identical. The odd samples are forwarded to path O and the even samples are forwarded to path E. The byte synchronizer is responsible for detecting the delimiter. It makes use of a payload detection algorithm to look for a preprogrammed delimiter. The idea behind the phase picking algorithm is to replicate the byte synchronizer twice in an attempt to detect the delimiter on either the odd and/or even samples of the data, respectively. That is, regardless of the phase step between two consecutive packets ($-2\pi \leq \Delta\varphi \leq +2\pi$ rads), there will be at least one clock edge (either t_{odd} or t_{even}) that will yield an accurate sample. The phase picker then uses feedback from the byte synchronizers to select the right path from the two possibilities. For further illustration, we refer the reader to the discussion in Sect. 4.3.

The realigned data are then sent to the RS(255, 239) decoder which is turned ON for the BER measurements with FEC; otherwise, it is bypassed (see Fig. 4). The RS decoder is an IP core from the Xilinx LogiCORE portfolio. The FPGA-based BERT designed in [10] is implemented to selectively perform BER and PLR measurements on only

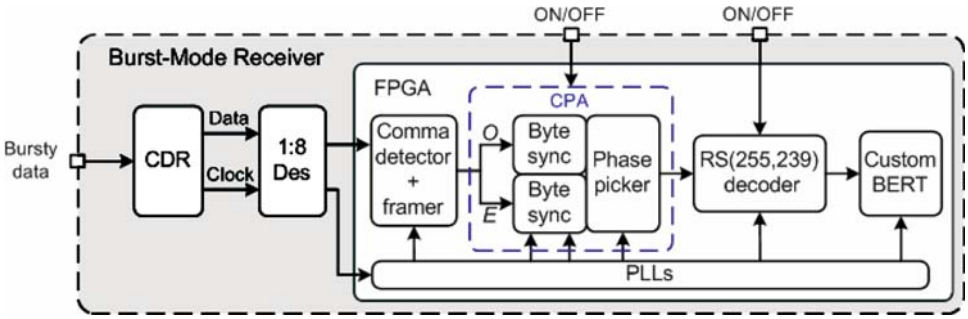

Fig. 4 Block diagram of the GPON OLT burst-mode receiver (CDR: clock-and-data recovery; Des: deserializer; CPA: clock phase aligner; PLL: phase-locked loop; BERT: bit-error rate tester)

the payload of the packets. The BERT compares the incoming data with an internally generated $2^{15} - 1$ PRBS. Note that, while a conventional BERT can be used to make the BER measurements, PLR measurements on discontinuous, bursty data, is not supported. This is because conventional BERTs require a continuous alignment between the incoming pattern and the reference pattern, and milliseconds to acquire synchronization. The phase step response of the burst-mode CDR can make conventional BERTs lose pattern synchronization at the beginning of every packet while the sampling clock is being recovered by the CDR. The custom BERT does not require fixed synchronization between the incoming pattern and the reference pattern of the error detector. Synchronization happens instantaneously at the beginning of every packet, therefore enabling PLR measurements on discontinuous, bursty data.

4 Experimental results and discussions

In this section, we experimentally study the effect of channel impairments on the performance of BMRx in the GPON uplink. The BMRx performance is quantified in terms of the BER and PLR measurements. More specifically, the following measurements are taken: BER versus signal power, PLR versus phase step, signal power, CID immunity, and BER. We also assess various tradeoffs and penalties in the preamble length, power budget, and pattern correlator error resistance. In addition, we investigate the impact of MPN in the uplink in terms of the effective PLR and BER coding gain. Where appropriate, comparisons between theoretical predictions and experimental results have been provided validating the analysis of the system. Finally, we present the results on dynamic burst-error correction.

4.1 Bit-error rate versus signal power

Current PON systems employ FP lasers at the ONU to minimize the cost per subscriber. However, the BER and PLR performance of the system may be severely impaired by the MPN of the FP laser. Thus, the G.984.2 standard [9] proposes the use of an 8-byte error-correcting FEC RS(255, 239) code to reduce the associated penalty. RS codes are a nonbinary subclass of multiple-error-correcting BCH codes [15]. The symbols of RS codes are elements of a Galois field $GF(q)$, where q is a power of some prime number. Both encoding and decoding of RS codes are performed at the symbol level and are based on Galois field arithmetic. Since elements in $GF(2^m)$ can easily be represented as binary vectors, in practice, RS codes defined over $GF(2^m)$ are generally used. A primitive $RS(n, k)$ code over $GF(2^m)$ has a block length of $n = 2^m - 1$, k of which are information symbols ($k < n$). A $RS(n, k)$ has a minimum distance $d = n - k + 1$ and thus it is called a maximum-distance-separable (MDS) code [15]. The MDS property and symbol-level encoding and decoding of RS codes make it an excellent candidate when both random and burst-error-correcting capabilities are required.

To study the impact of FEC on the optical link budget of the GPON uplink, we plot the BER performance with and without FEC, as a function of the received signal power as shown in Fig. 5. Note that the abscissa is the useful power, that is, the optical power contributed at the photodiode. We observe a coding gain of ~ 3 dB (measured at a BER $= 10^{-10}$). Note, according to the G.984.2 standard, coding gain is defined as the difference in input power at the receiver with and without FEC at a BER $= 10^{-10}$.

A comparison between the experimental and theoretical BER with FEC is shown in Fig. 5. Let p_e be the measured BER without FEC. Organizing the bits in symbols of m bits yields an equivalent symbol error rate p_S, under the assumption of purely random bit errors, as

$$p_S = 1 - (1 - p_e)^m \tag{2}$$

The $RS(n, k) = \mathrm{RS}(255, 239)$ block-based FEC code divides a codeword of n symbols into 8-bit symbols and k data (uncoded) symbols, yielding in a memoryless channel, a symbol error rate after FEC p_S^{FEC}, of [15]

$$p_S^{\mathrm{FEC}} \approx \frac{1}{2^m - 1} \sum_{j=t+1}^{2^m-1} j \binom{2^m - 1}{j} p_S^j (1 - p_S)^{2^m - 1 - j} \tag{3}$$

where

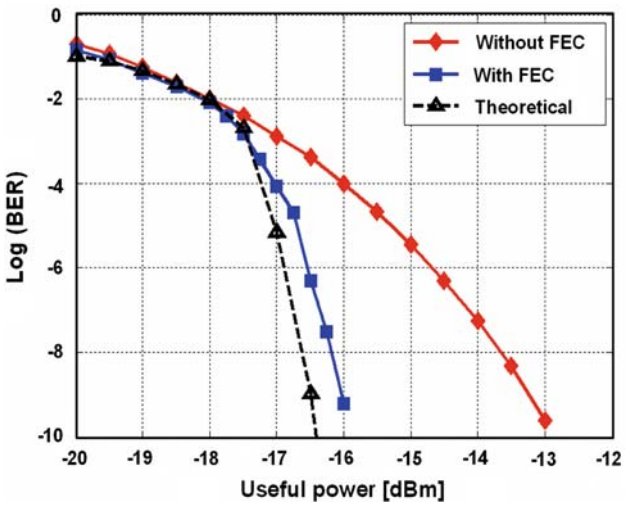

Fig. 5 BER versus signal power performance of the GPON uplink with and without FEC, and comparison to theoretical BER with FEC

$$t = \left\lfloor \frac{n-k}{2} \right\rfloor \tag{4}$$

and t is the symbol error correcting capability of the code. Note that $\lfloor x \rfloor$ represents the largest integer not to exceed x. Again, assuming a memoryless channel and since we are using orthogonal signaling (ON–OFF keying), the lower bound of the BER after FEC p_e^{FEC}, can be calculated as

$$p_e^{FEC} \geq \frac{p_S^{FEC}}{m} \tag{5}$$

We plot the purely random and memoryless channel prediction of the BER after FEC p_e^{FEC}, and our experimental results in Fig. 5. The BER performance is a function of intrinsic[1] and extrinsic[2] effects of the channel [16]. Thus, the presence of random and deterministic errors will affect the error correcting capability of the FEC code. It can be observed that the experimental and the theoretical results are in close agreement for BER $> 10^{-4}$. This is because for lower signal power, random errors dominate over deterministic errors in the system. However, for BER $< 10^{-4}$, we observe $\sim$0.5 dB of power penalty between the experimental and the theoretical results; our predictions are too optimistic. Since (2), (3), and (5) assume purely random bit errors and a memoryless channel, p_e^{FEC} is overestimated for BER $< 10^{-4}$. This is attributed to the fact that as the received power is increased, the presence of random errors is attenuated relative to the presence of deterministic errors. This is more likely due to the memory added in the channel through intensity noise, deterministic jitter, CDR, and other components, making the errors statistically dependent in a GPON uplink. An interleaver may be used to arrange the data in a non-contiguous way such that the codeword bits are interleaved before being transmitted. Thus, in the presence of deterministic jitter, only a correctable number of bits in each codeword will be affected. However, this increases latency.

[1] Intrinsic noise is unwanted random energy fluctuations of the signal electrons or photons caused by temperature, by the nonlinearity and gradient nonlinearity of the transmission medium, or by containments in the matrix of the medium; such noise is thermal, shot noise, and flicker or 1/f noise.

[2] Extrinsic noise is unwanted frequencies superimposed on the signal from external sources, such as electromagnetic interference, amplifier noise (ASE), cross talk, four-wave mixing, or detector noise.

4.2 Mode-partition noise analysis

MPN has been studied extensively in [17]. MPN is a phenomenon occurring because of an anti-correlation among pairs of longitudinal modes, that is, even though the total intensity of the modes remains relatively constant, various longitudinal modes fluctuate in such a way that individual modes exhibit large intensity fluctuations [8]. This leads to the different modes becoming unsynchronized because of group-velocity dispersion (GVD) as they travel at slightly different speeds inside the fiber. Thus, the SNR at the decision circuit becomes worse than that expected in the absence of MPN. Consequently, a power penalty must be paid to improve the SNR to the same value that is necessary to achieve the required BER. The power penalty caused by MPN existing in 1330 nm lightwave systems has been analyzed in [18].

Suppose the time average spectrum of the laser source is assumed to be Gaussian and the half spectrum width is σ_λ, then the mean square variance of MPN σ_{mpn}, is determined by [18]

$$\sigma_{mpn} = \frac{k}{\sqrt{2}}\left[1 - \exp\left(-\beta^2\right)\right] \tag{6}$$

where

$$\beta = \pi BDL\sigma_\lambda \tag{7}$$

and k is the mode-partition coefficient, B is the bit rate, D is the fiber delay dispersion per unit length per unit wavelength, and L is the length of the fiber. If MPN did not exist in the system, the signal power S_o which is required to achieve a given BER would be [19].

$$\frac{1}{Q^2} = \left(\frac{\sigma_o}{S_o}\right)^2 \tag{8}$$

where σ_o is the total receiver power and Q is determined by the BER p_e, as

$$p_e = \frac{1}{2}\mathrm{erfc}\left(\frac{Q}{\sqrt{2}}\right) \tag{9}$$

where

$$\operatorname{erfc}(x) = \frac{2}{\sqrt{\pi}} \int_{x}^{\infty} \exp\left(-\omega^2\right) d\omega \tag{10}$$

The required signal power S_m to achieve the same BER when MPN is added to the receiver noise becomes [19]

$$\frac{1}{Q^2} = \left(\frac{\sigma_o}{S_m}\right)^2 + \sigma_{mpn}^2 \tag{11}$$

and the resulting power penalty caused by MPN δ_{mpn}, is then [17]

$$\delta_{mpn} = 10 \log\left(\frac{S_m}{S_o}\right) = -5 \log\left(1 - Q^2 \sigma_{mpn}^2\right) \tag{12}$$

The coding gain G (when $\sigma_{mpn} = 0$) obtained by employing FEC will then also have to compensate for the power penalty δ_{mpn}, giving an MPN power penalty after FEC δ_{mpn}^{FEC}. Consequently, the effective coding gain G_{eff} (when $\sigma_{mpn} \neq 0$) of the system will decrease with an increase in MPN, giving a limitation on how much MPN can be tolerated in the GPON uplink. It can be expressed as

$$G_{eff}|_{\sigma_{mpn} \neq 0} = G|_{\sigma_{mpn}=0} - \delta_{mpn}^{FEC} \tag{13}$$

The relationship between G, G_{eff}, δ_{mpn}, and δ_{mpn}^{FEC}, is depicted in Fig. 6(a).

When the central wavelength of the laser used is within the zero dispersion window of the fiber (1302–1322 nm), in practice, no notable MPN penalty is observed even with the 20-km of uplink fiber [20]. However, we have performed simulations to account for the worst case scenario in the GPON uplink. Note that according to the G.984.2 standard [9], the ONU transmitter operating wavelength is specified in the 1260–1360-nm range.

In Fig. 6(b), we plot the BER with FEC and without FEC, for various values of the mean square variance of MPN σ_{mpn}. As expected, the system performance degrades with an increase in σ_{mpn}. More specifically, from Fig. 7(a) we observe that as the σ_{mpn} in the system increases, the coding gain penalty increases exponentially, while the effective coding gain decreases very rapidly. The maximum MPN that can be tolerated in the uplink giving an effective coding gain of zero, is when $\sigma_{mpn} \sim 0.14$.

Let us assume that the GPON uplink is a memoryless channel and that the presence of deterministic errors is negligible. According to the statistical analysis of MPN presented in [17, 18], MPN penalty in nearly single-mode lasers will lead to independent (random) errors. We can then use (2), (3), and (5) to estimate the theoretical bound when RS(255, 239) codes are employed to correct for the power penalty introduced by the MPN in the channel. In Fig. 7(b), we plot the BER performance of the system with and without FEC, and also the theoretical bound obtained for the worst case MPN when $\sigma_{mpn} = 0.14$. The effective coding gain is observed to be $\sim$3 dB. However, note that for $\sigma_{mpn} = 0.14$, we obtained an effective coding gain of zero from Fig. 7(a). This means that the 'extra' power penalty that we observed must be due to deterministic errors present in the GPON uplink.

4.3 Clock phase aligner discussion

The burst-mode functionality of the receiver is obtained by employing the CPA module. The CPA makes use of an oversampling CDR operating at 2× the bit rate and a phase picking algorithm. With the aid of some eye diagrams, we review the idea behind the phase picking algorithm in [10]. Figure 8 shows the response of the CDR to bursty traffic, as well as the 2× oversampling mode of the CDR and the CPA operation. Three specific phase differences between packets are considered: (a) no phase difference $\Delta\varphi = 0$ rad (0 ps); (b) $\Delta\varphi = \pi/2$ rads (400 ps); and $\Delta\varphi = \pi$ rads (800 ps). Note, whereas $\Delta\varphi = \pi$ rads (800 ps) represents a worst case phase step for the CDR operated at the bit rate (see Fig. 8(f)), $\Delta\varphi = \pi/2$ rads (400 ps) phase step is the worst case scenario for the oversampling CDR at 2× the bit rate (see Fig. 8(h)).

The 2× oversampling mode produces two samples per bit, which helps the CPA algorithm to lock at the correct

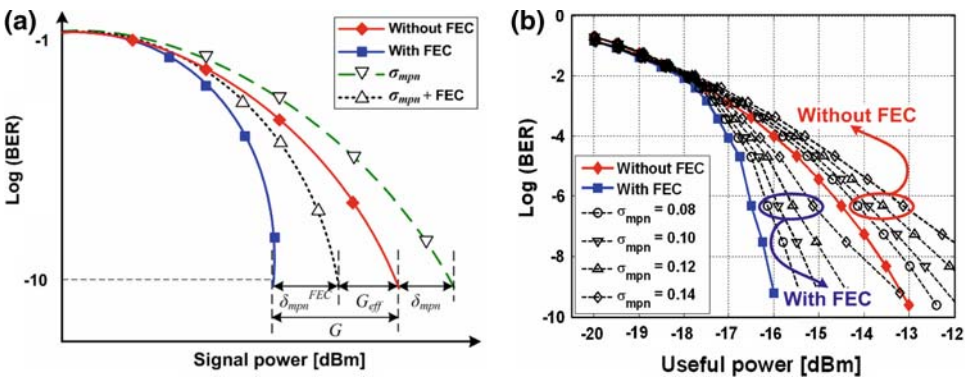

Fig. 6 (**a**) Graphical depiction of the relationships between coding gain, effective coding gain, and MPN penalty before and after FEC. (**b**) BER versus signal power for various MPN mean square variances in GPON uplink

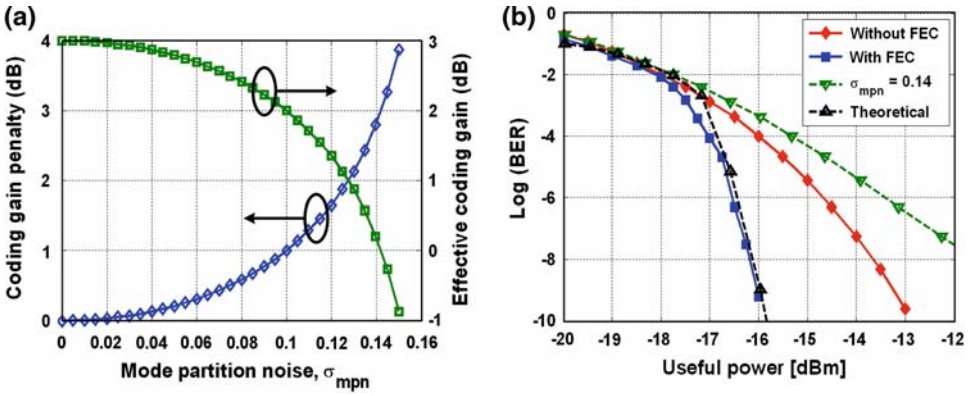

Fig. 7 (**a**) Effective coding gain and MPN penalty after FEC versus mean square variance of MPN. (**b**) Theoretical determination of effective coding gain with the worst-case MPN assuming only random errors in GPON uplink

phase of the incoming packet. To understand how the CPA works, consider the case when there is no phase step ($\Delta\varphi = 0$ rad); path O correctly samples the incoming pattern (see t_{odd} in Fig. 8(g)). For phase step $\Delta\varphi = \pi/2$ (400 ps) rads, path E will sample the bits on or close to the transitions after the phase step (see t_{even} in Fig. 8(h)). In this situation, the byte synchronizer of path E will likely not detect the delimiter at the beginning of the packet. On the other hand, the byte synchronizer of path O will have no problems detecting the delimiter (see t_{odd} in Fig. 8(h)). The phase picker controller monitors the state of the two byte synchronizers and selects the correct path accordingly (path O in this particular case). Once the selection is made, it cannot be overwritten until the comma is detected, indicating the end of the packet. This process repeats itself at the beginning of every packet. The result is that the CPA achieves instantaneous phase acquisition (0-bit) for any phase step ($\pm 2\pi$ rads), that is, no preamble bits at the beginning of the packet are necessary. We further discuss these results in the next section.

4.4 Packet-loss ratio versus phase step

In this section, we investigate the PLR performance of the GPON uplink as a function of the phase step between consecutive packets. Let us first consider the case for a back-to-back configuration (without the 20-km of uplink fiber). Figure 9(a) shows PLR versus phase step performance, with only the CDR and the CPA turned off. We have restricted the horizontal axis to values from $0 \leq \Delta\varphi \leq 1600$ ps, corresponding to $0 \leq \Delta\varphi \leq 2\pi$ rads phase difference at the desired bit rate ($\sim$622 Mb/s). Also, note that the results are symmetrical about 0 rad from $-2\pi \leq \Delta\varphi \leq 0$ rads. We observe a bell-shaped curve centered at 800 ps because this represents the half bit period corresponding to the worst-case phase step at $\Delta\varphi = \pi$ rads, and therefore, the CDR is sampling exactly at the edge of the data eye. Jitter would have led to the worst case phase (π rad) being displaced from 800 ps. Hence, we conclude that jitter is not significant in our measurements. At relatively small phase shifts (near 0 or

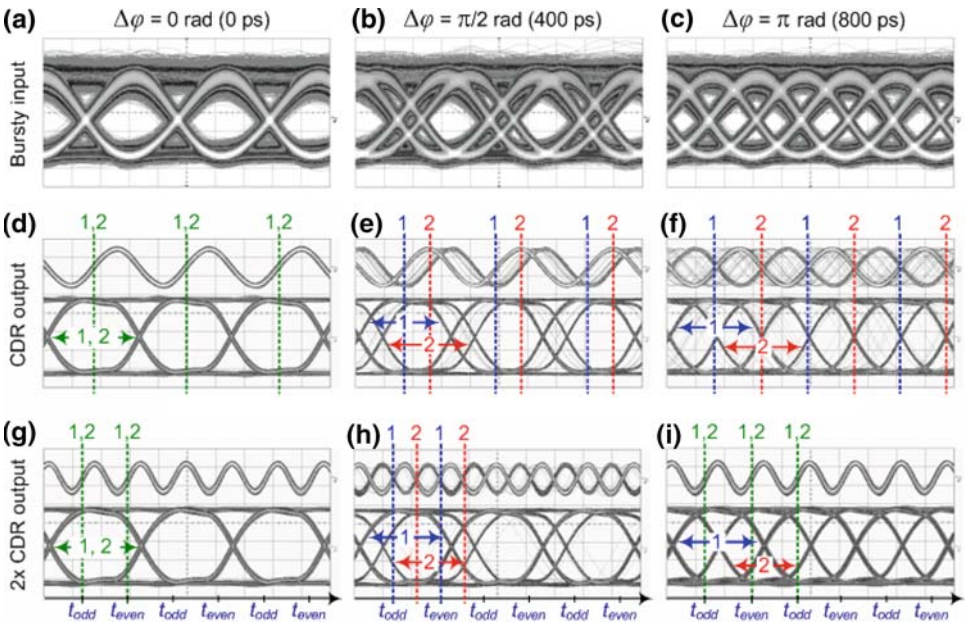

Fig. 8 (**a–c**) Bursty traffic (packets with different phases) input signal to the receiver with phase steps: $\Delta\varphi = 0$ rad (0 ps), $\Delta\varphi = \pi/2$ rads (400 ps), and $\Delta\varphi = \pi$ rads (800 ps). (**d–f**) Response of the CDR to bursty traffic. (**g–i**) Response of the 2× oversampling CDR to bursty traffic and the depiction of the odd and even samples resulting from t_{odd} and t_{even} sampling instants

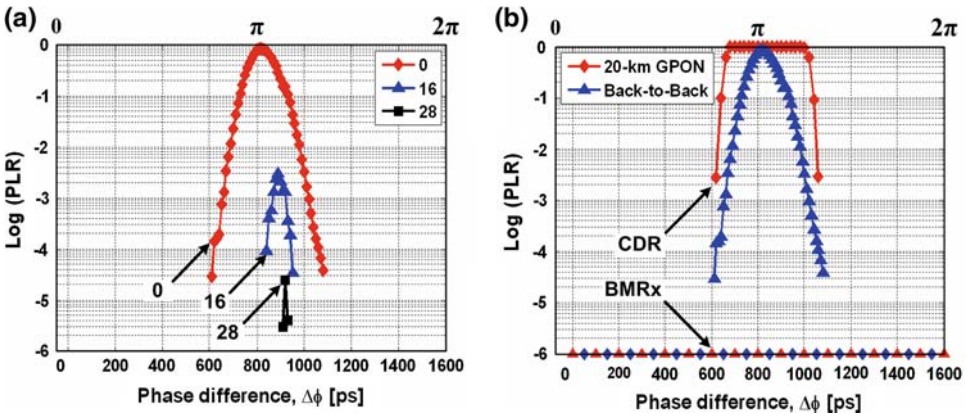

Fig. 9 PLR versus phase step performance of GPON uplink. (**a**) Back-to-back configuration with CDR for different preamble lengths. (**b**) Comparison between 20 km GPON and back-to-back configurations with and without BMRx for no preamble

2π rad), we can easily achieve zero PLR with the CPA module disabled because the CDR is almost sampling at the middle of each bit (refer to Fig. 8(a)).

Preamble bits ("1010…" pattern) can be inserted at the beginning of the packets to help the CDR settle down and acquire lock. As the preamble length is increased, there is an improvement in the PLR. After 32 preamble bits, we observe error-free operation (PLR $< 10^{-6}$) for any phase step. There are two comments on this. First, the use of the preamble reduces the effective throughput and increases delay. Second, this preamble length of 32 bits does not satisfy the 28-bit requirement specified in the G.984.2 standard [9]. Moreover, assuming 2 bytes of the preamble are reserved for amplitude recovery, this leaves only 12 bits for phase recovery [6].

With the introduction of a 20-km communication fiber link, there is a degradation in the PLR performance as the worst-case PLR spans a wider range of phase steps as depicted in Fig. 9(b). However, by switching on the burst-mode functionality of the receiver with the CPA, we observe error-free operation in both configurations for any phase step ($0 \leq \Delta\varphi \leq 2\pi$ rads) with *no* preamble bits, allowing for instantaneous phase acquisition. This is well below the maximum preamble length of 28 bits specified in the GPON standard. We note that a sensitivity penalty results from the quick extraction of the decision threshold and clock phase from a short preamble at the start of each packet [12, 13]. However, by reducing the length of the CPA field, as demonstrated in this work, more bits are left for amplitude recovery, thus reducing the burst-mode sensitivity penalty. Alternatively, with the reduced number of preamble bits, more bits can be left for the payload, thereby increasing the information rate.

4.5 Packet-loss ratio versus signal power

The PLR performance of the GPON uplink as a function of the received signal power is shown in Fig. 10. Again, note that the abscissa is the useful power, that is, the optical power contributed at the photodiode. To determine the burst-mode penalty of the receiver, consider the plot in Fig. 10(a). The PLR performance of the CDR sampling continuous data at the bit rate with no phase difference ($\Delta\varphi = 0$ rad), is compared to the PLR performance of the BMRx (with CPA) sampling bursty data with the worst-case phase difference ($\Delta\varphi = \pi/2$ rads). Both measurements are made for a 0-bit preamble. We observe a penalty of less than 1 dB, due to the $2\times$ oversampling (faster electronics) and the phase picking algorithm. The respective eye diagrams at the input of the BMRx are shown as insets.

If there is a worst-case phase difference between consecutive packets in the GPON uplink, the CDR will not be able to recover any packets, regardless of the signal power, resulting in a PLR $\sim$ 1 as shown in Fig. 10(b). However, if the GPON standard of a 28-bit preamble is complied

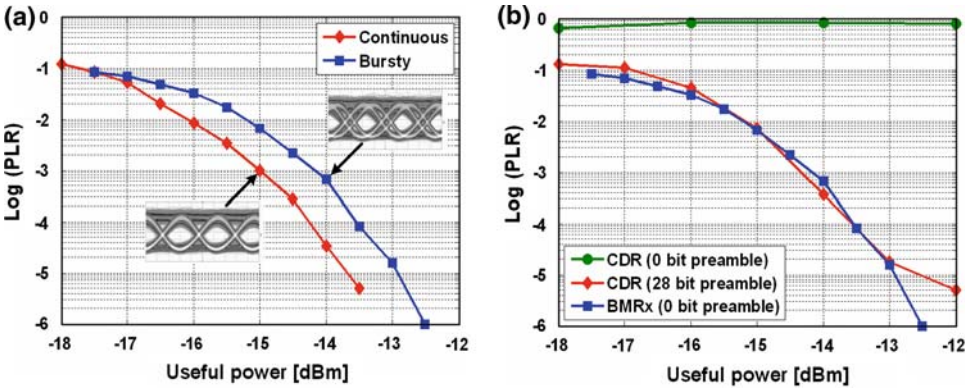

Fig. 10 PLR versus signal power performance of GPON uplink. (**a**) Burst-mode penalty by comparing continuous-mode and burst-mode reception by CDR and BMRx, respectively. (**b**) Preamble length penalty comparing BMRx with 0-bit preamble and CDR with 0-bit and 28-bit preambles

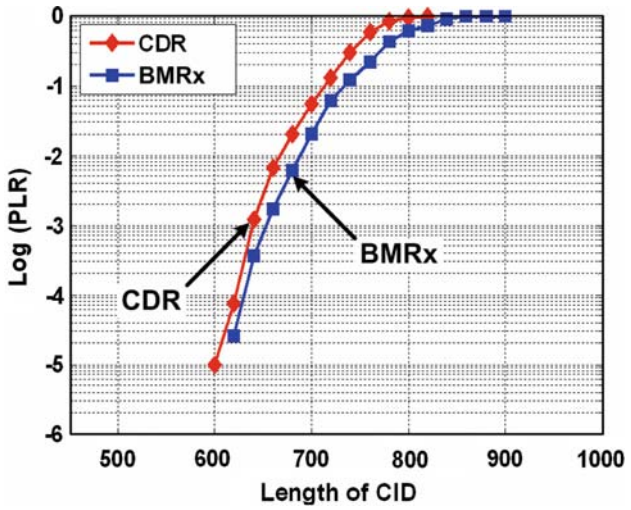

Fig. 11 PLR versus CID immunity performance in GPON uplink

with, the PLR performance of the CDR is then comparable to the PLR performance obtained by the BMRx which does not require any preamble bits. Hence, there is a tradeoff between the power penalty with the BMRx oversampling when $\Delta\varphi = 0$ rad and the number of preamble bits required without the BMRx when $\Delta\varphi \neq 0$ rad. Since phase steps between consecutive packets in the GPON uplink are inevitable, the 1-dB power penalty may be a small price to pay than not receiving any packets at all.

4.6 Packet-loss ratio versus CID immunity

We measure the CID immunity of the BMRx by zeroing bits at the end of packet 1 until error-free operation (PLR $< 10^{-6}$ and BER $< 10^{-10}$) can no longer be maintained on packet 2. The phase step and the preamble length are both set to zero for this measurement. The CID immunity of the receiver is depicted in Fig. 11. It can be seen that the receiver can support $\sim$600 CIDs with error-free operation. This is eight times more than the minimum allowed number of CIDs specified in G.984.2, which is 72 bits [9].

4.7 Packet-loss ratio versus bit-error rate and mode-partition noise

A delimiter of a packet that cannot be detected correctly will lead to the packet being lost, and thus contribute to the PLR. The error resistance of the delimiter depends not only on its length, but also on the exact implementation of the pattern correlator. Let PLR_z represent the PLR obtained at a given BER of p_e with a pattern correlator having an error resistance of z bits in a d-bit delimiter. The PLR_z can then be estimated as

$$\mathrm{PLR}_z \leq \sum_{j=z+1}^{d} P(j) \approx P(z+1) \text{ for } p_\mathrm{e} \ll 1 \tag{14}$$

where

$$P(x) = \binom{d}{x} p_\mathrm{e}^x (1-p_\mathrm{e})^{d-x} \tag{15}$$

$P(x)$ gives the probability of finding x errors out of a d-bit delimiter given that the probability of finding a bit error is p_e. In Fig. 12(a), we compare experimentally and theoretically, the PLR performance of the GPON uplink as a function of the received signal power. Our experimental results and the theoretical predictions are in very close agreement albeit a negligible penalty of $\sim$0.1 dB. This penalty may be explained by the assumptions that (14) is based on, which include: (1) the errors in the delimiter of the packet follow a binomial distribution, and (2) the probability of these errors is given by the BER of the system. The latter is only true in the case of purely random errors, which clearly, may not be the case.

The complexity of the pattern correlator depends on an acceptable error resistance of the delimiter. Consider the plot in Fig. 12(b) which shows the PLR performance as a function of the BER for various pattern correlator error resistance values of the delimiter. Even with a simple pattern correlator having $z = 1$ bit error resistance, we obtain error-free operation: PLR $< 10^{-9}$ at BER $= 10^{-10}$. Furthermore, by increasing the pattern correlator error

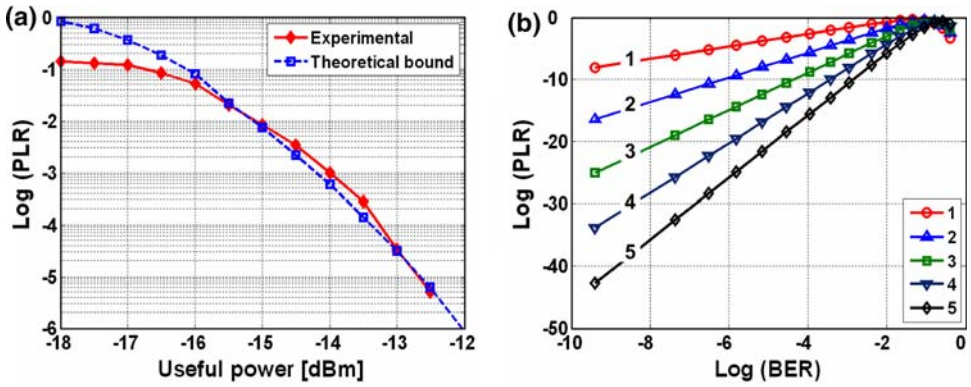

Fig. 12 (**a**) Comparison between theoretical and measured PLR versus signal power. (**b**) PLR versus BER performance with a pattern correlator having different error resistance values in a delimiter

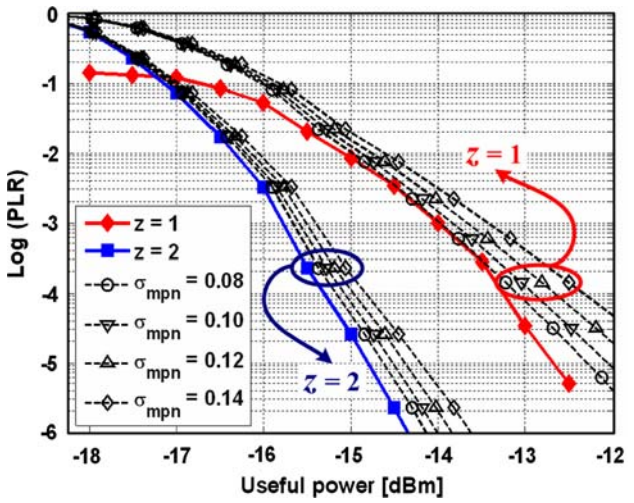

Fig. 13 PLR versus signal power for different MPN mean square variances in GPON uplink

resistance to $z = 2$ bits, we obtain improvement in the PLR performance by eight orders of magnitude.

In Sect. 4.2, we studied the effect of MPN on the uplink in terms of the BER performance of the system. It is also interesting to see the effect that MPN has on the PLR performance of the system. In Fig. 13, we plot the PLR for various values of the mean square variance of MPN σ_{mpn}. As expected, the system performance degrades with an increase in σ_{mpn}. Recall that the maximum MPN that can be tolerated in the uplink giving an effective coding gain of zero, is when $\sigma_{\text{mpn}} \sim 0.14$. At this value of MPN, there is a deterioration of more than two orders of magnitude in the PLR for signal power ≥ -13 dBm. However, by increasing the pattern correlator error resistance to $z = 2$ bits, we observe a coding gain of $\sim$2 dB at a PLR $= 10^{-6}$ which can be used to compensate for the MPN penalty and also the 1-dB burst-mode penalty (see Fig. 10(a)).

4.8 Dynamic burst-error correction

A burst-error is defined as an n-bit sequence that contains clustered bit errors. Two erroneous bits always mark the first and last bits of the sequence, and there can be any number of errors, up to $(n - 2)$, in between them [21]. Burst-errors inherently arise in GPON uplink because of the phase acquisition process by CDRs for bursty data. This makes the BER measurements unreliable and unpredictable, and therefore not a true representation of BER. There are two comments on this. First, at a particular signal power, the BER may not converge because of the presence of burst-errors from packet to packet. Thus, the BER can change from measurement to measurement for the same signal power. Second, the BER will also vary for packets with different phases at the same signal power. This is because the phase acquisition time of the CDR is a function of the relative phase difference between two packets.

RS codes can be useful for burst-error correction provided that the burst length is less than the codes' error correcting capability 0. However, there is no such guarantee in a GPON uplink because the signal power and the phase difference between packets vary in burst-mode reception from packet to packet. Burst-error correcting codes have been demonstrated for bursty channels [22–26], but these codes introduce complexity at the circuit level implementation. On the other hand, RS codes are relatively simple. Our technique of employing FEC with RS codes in a BMRx with fast phase acquisition provides a simple solution to correct for burst-errors in a GPON uplink.

In Fig. 14, the BER and the PLR performance of the system is monitored as function of packet reception. Let us first consider the case with the CPA and FEC turned off (see Fig. 14(a)), and the signal power is such that the BER $= 10^{-4}$. Starting with no phase difference between the consecutive packets $\Delta\varphi = 0$ rad and switching the FEC on, the RS(255, 239) codes help obtain a BER $= 10^{-10}$ as expected. However, with a phase step $\Delta\varphi \neq 0$ rad introduced in the uplink, the following can happen: first, the phase difference can result in a poor PLR with almost all the packets being lost as shown in Fig. 14(b). Note that BER measurements can only be made on packets that are received. This means that with almost all packets lost, the BER obtained will be unreliable. A packet lost may be

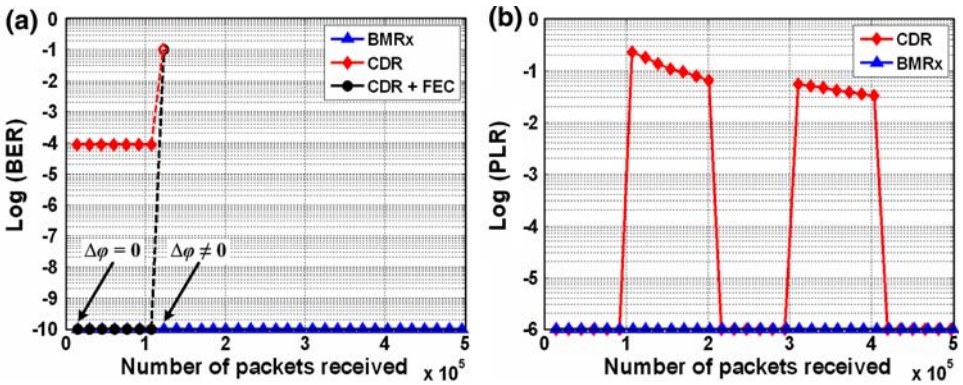

Fig. 14 BER and PLR performance versus number of received packets in GPON uplink

retransmitted. However, despite any number of retransmissions, there is no guarantee that the packets will be received as the PLR $\sim$ 1. Second, even if the packet is received, that is the delimiter can be detected, the introduction of the phase step, will induce a severely errored burst whose length is much larger than the error correcting capability of the RS codes. As depicted in Fig. 12(b), for PLR $\sim$ 1, the BER $> 10^{-1}$ regardless of the error resistance of the pattern correlator on the delimiter. As long as the burst length is not more than the error correcting capability of the RS code (BER $< 10^{-4}$), the errors can be corrected. Clearly this is not the case here.

We perform similar tests on the BMRx with the CPA and FEC turned on. It can be observed from Fig. 14 that regardless of a phase step introduced in the uplink, no packets are lost because of the ability of the CPA to instantaneously acquire the phase. Thus, the BER does not vary for packets with different phase and no burst of errors are introduced, making the task of the RS(255, 239) codes easy to bring down the BER $< 10^{-10}$, leading to reliable and predictable BER measurements.

5 Summary and conclusion

We experimentally investigated the effect of channel impairments on the performance of a BMRx in a 622 Mb/s 20-km GPON uplink, and quantified the results in terms of the BER and PLR performance of the system. Our receiver features a CPA for automatic phase acquisition, and an RS (255, 239) decoder for FEC. The CPA makes use of a phase picking algorithm and an oversampling CDR operated at 2$\times$ the bit rate.

This BMRx provides instantaneous (0 preamble bit) phase acquisition with PLR $< 10^{-6}$ and BER $< 10^{-10}$ for any phase step ($\pm 2\pi$ rads) between consecutive packets, clearly meeting the 28-bit preamble specification of GPON. The receiver also supports more than 600 CIDs, which is eight times more than the minimum 72-bit GPON specification. By reducing the length of the CPA field, more bits are left for amplitude recovery, thus, reducing the burst-mode sensitivity penalty. Alternatively, with the reduced number of preamble bits, more bits can be left for the payload, thereby increasing the information rate, and thus, the effective system throughput. The price to pay, a 1-dB power penalty, to obtain instantaneous phase acquisition is faster electronics. On the other hand, our solution leverages the design of components for long-haul transport networks. These components are typically a generation ahead of the components for multi-access networks. Thus, our solution will scale with the scaling for long-haul networks. It should be noted here that off-the-shelf components for RS codes are available for throughput below 1 Gb/s. However, with the scaling of GPON data rates as they reach 10 Gb/s and beyond, the power consumption and complexity of these FEC devices will be the main barrier to integrate them into optical communication systems at low cost [27]. The 622 Mb/s BMRx inherits the low jitter transfer bandwidth (1 MHz) and the low jitter peaking (0.1 dB) of the oversampling CDR at 1.25 Gb/s. Hence, this receiver could also find applications in burst/packet switched networks, which may require a cascade of BMRx that each consumes some of the overall jitter budget of the system.

The receiver also accomplishes a 3-dB coding gain at BER $= 10^{-10}$. The coding gain can be used to reduce the minimum and maximum transmitter power, or increase the minimum receiver sensitivity by the same amount. Alternatively, the effective coding gain can be used to reduce the penalty due to MPN, and thus achieve a longer physical reach or support more splits per single PON tree. We observed a power penalty of 0.5 dB between the experimental and the theoretical BER results with FEC. The penalty is due to the memory added in the channel and the presence of deterministic burst-errors. As stated earlier, the theoretical analysis assumes purely random bit errors and a memoryless channel.

We also studied the impact of MPN in the GPON uplink in terms of the BER and the PLR performance of the system. As the MPN in the system increases, the coding gain penalty increases exponentially, while the effective coding gain decreases very rapidly. The maximum MPN that can be tolerated in the uplink giving an effective coding gain of zero, is when $\sigma_{\text{mpn}} = 0.14$. At this value, there is a deterioration of more than two orders of magnitude in the PLR for signal power ≥ -13 dBm.

We showed that the experimental results and the theoretical PLR performance of the system are in good agreement. Furthermore, we analyzed the PLR performance as a function of the BER and the pattern correlator error resistance of the delimiter. A BMRx with a simple pattern correlator having a 1-bit error resistance obtains error-free operation with PLR $< 10^{-9}$ at BER $= 10^{-10}$. By increasing the pattern correlator error resistance to 2 bits, the PLR performance can be improved by eight orders of magnitude. In addition, we observed a coding gain of $\sim$2 dB at a PLR $= 10^{-6}$ which can be used to compensate for the penalty introduced by the MPN, and also the 1-dB burst-mode penalty.

Finally, we addressed the problem of monitoring BERs in bursty GPON uplink. We demonstrated how the CPA and the RS(255, 239) codes can be used in tandem for dynamic burst-error correction, giving reliable BERs in bursty channels.

Acknowledgments This work was supported in part by National Sciences and Engineering Research Council of Canada (NSERC)

through the Alexander Graham Bell Canada Graduate Scholarship (CGS), McGill University through the Lorne Trottier Engineering Fellowship and McGill Engineering Doctoral Award (MEDA), Le Fonds Québécois de la Recherche sur la Nature et les Technologies (FQRNT) through graduate scholarships, by industrial and government partners through the Bell Canada NSERC Industrial Research Chair (IRC), the NSERC-funded Agile All-Photonic Networks (AAPN) Research Network, and by the Canadian Institute for Photonic Innovation (CIPI).

References

1. Girard, A. (2005). *FTTx PON technology and testing*. Quebec City, QC, Canada: Electro-Optical Engineering Inc., 1-55342-006-3.
2. Lee, C.-H., Sorin, W. V., & Kim, B. Y. (2006). Fiber to the home using a PON infrastructure. *IEEE Journal of Lightwave Technology, 24*(12), 4568–4583.
3. Abrams, M., Becker, P. C., Fujimoto, Y., O'Byrne, V., & Piehler, D. (2005). FTTP deployments in the United States and Japan-equipment choices and service provider imperatives. *IEEE Journal of Lightwave Technology, 23*(1), 236–246.
4. Wagner, R. E., Igel, J. R., Whitman, R., Vaughn, M. D., Ruffin, A. B., & Bickham, S. (2006). Fiber based broadband-access deployment in the United States. *IEEE Journal of Lightwave Technology, 24*(12), 4526–4540.
5. Koonen, T. (2006). Fiber to the home/fiber to the premises: What, where, and when. *Proceedings of the IEEE, 94*(5), 911–934.
6. Qiu, X.-Z., Ossieur, P., Bauwelinck, J., Yi, Y., Verhulst, D., Vandewege, J., et al. (2004). Development of GPON upstream physical-media-dependent prototypes. *IEEE Journal of Lightwave Technology, 22*(11), 2498–2508.
7. Oh, Y.-H., Lee, S.-G., Le, Q., Kang, H.-Y., & Yoo, T.-W. (2005). A CMOS burst-mode optical transmitter for 1.25-Gb/s ethernet PON applications. *IEEE Transactions on Circuits and Systems II: Express Briefs, 52*(11), 780–783.
8. Agrawal, G. P. (2002). *Fiber-optic communication systems* (3rd ed.). New York, NJ: John Wiley & Sons.
9. Gigabit-capable Passive Optical Networks (GPON). (2003). *Physical media dependent (PMD) layer specification*, ITU-T Recommendation G.984.2.
10. Faucher, J., Mukadam, M. Y., Li, A., & Plant, D. V. (2006). 622/1244 Mb/s burst-mode CDR for GPONs. In *Proceedings of IEEE Laser and Electro-Optics Society (LEOS) Annual Meeting*, Montreal, QC, Canada, October, Paper TuDD3.
11. Shastri, B. J., Faucher, J., Zeng, M., & Plant, D. V. (2007). Burst-mode clock and data recovery with FEC and Fast phase acquisition for burst-error correction in GPONs. In *Proceedings of IEEE Midwest Symposium on Circuits and Systems (MWSCAS)*, Montreal, QC, Canada, August, pp. 120–123.
12. Eldering, C. A. (1993). Theoretical determination of sensitivity penalty for burst mode fiber optic receivers. *IEEE Journal of Lightwave Technology, 11*(12), 2145–2149.
13. Ossieur, P., Qiu, X.-Z., Bauwelinck, J., & Vandewege, J. (2003). Sensitivity penalty calculation for burst-mode receivers using avalanche photodiodes. *IEEE Journal of Lightwave Technology, 21*(11), 2565–2575.
14. Goodman, J. W. (2000). *Statistical optics*. New York, NJ: Wiley.
15. Sklar, B. (2001). *Digital communications: fundamentals and applications* (2nd ed.). Upper Saddle River, NJ: Prentice-Hall.
16. Kartalopoulos, S. V. (2004). *Optical bit error rate: an estimation methodology*. New York, NJ: Wiley.
17. Ogawa, K. (1982). Analysis of mode partition noise in laser transmission systems. *IEEE Journal of Quantum Electronics, 18*(5), 849–855.
18. Agrawal, G. P., Anthony, P. J., & Shen, T. M. (1988). Dispersion penalty for 1.3-μm lightwave systems with multimode semiconductor lasers. *IEEE Journal of Lightwave Technology, 6*(5), 620–625.
19. Liu, X., Lu, C., & Cheng, T. H. (2005). Forward error control in passive optical networks. In *Proceedings of Optical Fiber Communication (OFC) Conference*, Vol. 1, Anaheim, CA, March, p 3.
20. Yi, Y., Verschuere, S., Lou, Z., Ossieur, P., Bauwelinck, J., Qiu, X.-Z., et al. (2008). Simulations and experiments on the effective optical gain of FEC in a GPON uplink. *IEEE Photonics Technology Letters, 19*(2), 82–84.
21. Jagath-Kumara, K. D. R., & Bebbington, M. (2005). Error content in frames transmitted over burst-error channels. *IEEE Transactions Wireless Communications, 4*(5), 2533–2539.
22. Hagelbarger, D. W. (1959). Recurrent codes: easily mechanized, burst-correcting, binary codes. *Bell Systems Technical Journal, 38*, 969–984.
23. Wadare, I. (1968). On type-B1 burst-error-correcting convolutional codes. *IEEE Transactions on Information Theory, 14*(4), 577–583.
24. Berlekamp, E. R. (1964). Notes on recurrent codes. *IEEE Transactions on Information Theory, 10*(3), 257–258.
25. Preparata, F. P. (1964). Systematic construction of optimal linear recurrent codes for burst error correction. *Calcolo, 1*(2), 147–153.
26. Kohlenberg, A., & Forney, G., Jr. (1968). Convolutional coding for channels with memory. *IEEE Transactions on Information Theory, 14*(5), 618–626.
27. Song, L., Yu, M.-L., & Shaffer, M. S. (2002). 10- and 40-Gb/s forward error correction devices for optical communications. *IEEE Journal of Solid-State Circuits, 37*(11), 1565–1573.

Bhavin J. Shastri was born in Nairobi, Kenya in 1981. He received the Honors B. Eng. (with distinction) and M. Eng. degrees in Electrical and Software Engineering from McGill University, Montreal, QC, Canada, in 2005 and 2007, respectively. He is currently working toward the Ph.D. degree in Electrical Engineering at the Photonic Systems Group of McGill University. He worked as a Wireless Systems Engineer at InterDigital Communications Corporation, QC, Canada, during his internship year in 2003. During 2002–2004, he worked as a Research Assistant at the Center for Intelligent Machines (CIM), McGill University and VisionSphere Technologies Inc., QC, Canada, developing face recognition systems. His research interests include high-speed burst-mode optical receivers, passive optical networks (PONs), optoelectronic-VLSI systems, image processing, and computer vision. Mr. Shastri is the recipient of the prestigious Alexander Graham Bell Canada Graduate Scholarship (2008) from the National Sciences and Engineering Research Council of Canada (NSERC). He is a Lorne Trottier Engineering Graduate Fellow, and the recipient of the McGill Engineering Doctoral Award (2007). Recently, he won two Best Student Poster Awards at the Canadian Institute for Photonic Innovation (CIPI) Annual Workshops (2008, 2007), and was awarded the IEEE Laser and Electro-Optics Society (LEOS) Travel Grant (2007). He is also the recipient of the IEEE Computer Society Lance Stafford Larson Outstanding Student Award (2004), the IEEE Canada Life Member Award for the Best Student Paper (2003), the James McGill Award (2005) and the Faculty of Engineering Award (2001) for being ranked in

the top 5%. He is a reviewer for the *Computer Vision and Image Understanding (CVIU) Journal* and *Machine Vision and Applications (MVA) Journal*, a student member of IEEE-LEOS and the Optical Society of America (OSA), and the current Vice-President of the McGill OSA Student Chapter.

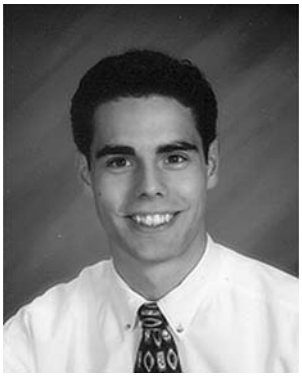

Julien Faucher received the Ph.D. degree in Electrical Engineering from McGill University, Montreal, Canada, in 2006. He has been working at PMC-Sierra, in the mixed-signal group, since 2005. His research interests include burst-mode receivers, clock and data recovery circuits, and mixed-signal design and verification. Dr. Faucher received graduate scholarships from the Natural Sciences and Engineering Research Council of Canada (NSERC) and from Le Fonds pourla Formation de Chercheurs et l'Aide à la Recherche du Québec (FCAR). He was also awarded a Richard H. Tomlinson Doctoral Fellowship from McGill University.

Noha Kheder was born in Cairo, Egypt. She received the B. Eng. degree (with distinction) in Electrical Engineering from McGill University, Montreal, QC, Canada, in 2006, where she is currently working toward the M.Eng. degree in Electrical Engineering. Her research interests include passive optical networks and burst-mode receivers for passive optical networks. Ms. Kheder is the recipient of a Master's research scholarship from Le Fonds Quebecois de la Recherche sur la Nature et les Technologies (FQRNT). She is the current Vice President of the IEEE McGill Student Branch.

Ming Zeng was born in Wuhan, China in 1983. She received the B. Eng. honors degree in Electrical Engineering from McGill University, Montreal, QC, Canada in 2007, where she is working toward the M.Eng. degree in Electrical Engineering. Since 2006, she has been working with the Photonic Systems Group, Department of Electrical and Computer Engineering, McGill University, where she completed her undergraduate thesis on burst-mode receiver for passive optical network. She is the current President of IEEE McGill Student Branch.

Nicholas Zicha was born in Montreal, Canada in 1981. He received his Honors B. Eng (with distinction) in Electrical Engineering from McGill University, Montreal, Canada in 2004. After working in industry as a digital hardware designer, he is currently pursuing his M. Eng. degree in Electrical Engineering at McGill University. His research interests include high-speed burst-mode optical receivers, high-speed inter-chip communications, and optoelectronic-VLSI systems.

David V. Plant received the Ph.D. degree in Electrical Engineering from Brown University, Providence, RI, in 1989. From 1989 to 1993, he was a Research Engineer at the Department of Electrical and Computer Engineering, University of California at Los Angeles (UCLA). He has been a Professor and Member of the Photonic Systems Group, the Department of Electrical and Computer Engineering, McGill University, Montreal, QC, Canada, since 1993, and Chair of the Department since 2006. He is the Director and Principal Investigator of the Centre for Advanced Systems and Technologies Communications at McGill University. During the 2000–2001 academic years, he took a leave of absence from McGill University to become the Director of Optical Integration at Accelight Networks, Pittsburgh, PA. His research interests include optoelectronic-VLSI, analog circuits for communications, electro-optic switching devices, and optical network design including OCDMA, radio-over-fiber, and agile packet switched networks. Dr. Plant has received five teaching awards from McGill University, including most recently the Principal's Prize for Teaching Excellence in 2006. He is a James McGill Professor and an IEEE LEOS Distinguished Lecturer. He was the recipient of the R.A. Fessenden Medal and the Outstanding Educator Award, both from IEEE Canada, and received a NSERC Synergy Award for Innovation. He is a member of Sigma Xi, a Fellow of Optical Society of America, and a Fellow of the IEEE.